

University of Wollongong

Research Online

Australian Institute for Innovative Materials -
Papers

Australian Institute for Innovative Materials

1-1-2016

Evaluation of persistent-mode operation in a superconducting MgB₂ coil in solid nitrogen

Dipakkumar Patel

University of Wollongong, djp485@uowmail.edu.au

Md Shahriar Hossain

University of Wollongong, shahriar@uow.edu.au

Khay Wai W. See

University of Wollongong, kwsee@uow.edu.au

Wenbin Qiu

University of Wollongong, wq118@uowmail.edu.au

Hiroki Kobayashi

University of Wollongong

See next page for additional authors

Follow this and additional works at: <https://ro.uow.edu.au/aiimpapers>

 Part of the [Engineering Commons](#), and the [Physical Sciences and Mathematics Commons](#)

Recommended Citation

Patel, Dipakkumar; Hossain, Md Shahriar; See, Khay Wai W.; Qiu, Wenbin; Kobayashi, Hiroki; Ma, Zongqing; Kim, Seong Jun; Hong, Jonggi; Park, Jin Yong; Choi, Seyong; Maeda, Minoru; Shahabuddin, Mohammed; Rindfleisch, Matthew A.; Tomsic, Michael; Dou, S X.; and Kim, Jung Ho, "Evaluation of persistent-mode operation in a superconducting MgB₂ coil in solid nitrogen" (2016). *Australian Institute for Innovative Materials - Papers*. 1750.

<https://ro.uow.edu.au/aiimpapers/1750>

Research Online is the open access institutional repository for the University of Wollongong. For further information contact the UOW Library: research-pubs@uow.edu.au

Evaluation of persistent-mode operation in a superconducting MgB₂ coil in solid nitrogen

Abstract

We report the fabrication of a magnesium diboride (MgB₂) coil and evaluate its persistent-mode operation in a system cooled by a cryocooler with solid nitrogen (SN₂) as a cooling medium. The main purpose of SN₂ was to increase enthalpy of the cold mass. For this work, an in situ processed carbon-doped MgB₂ wire was used. The coil was wound on a stainless steel former in a single layer (22 turns), with an inner diameter of 109 mm and height of 20 mm without any insulation. The two ends of the coil were then joined to make a persistent-current switch to obtain the persistent-current mode. After a heat treatment, the whole coil was installed in the SN₂ chamber. During operation, the resultant total circuit resistance was estimated to be $<7.4 \times 10^{-14} \Omega$ at $19.5 \text{ K} \pm 1.5 \text{ K}$, which meets the technical requirement for magnetic resonance imaging application.

Keywords

solid, evaluation, persistent, mode, operation, superconducting, mgb₂, coil, nitrogen

Disciplines

Engineering | Physical Sciences and Mathematics

Publication Details

Patel, D., Hossain, M. Al., See, K., Qiu, W., Kobayashi, H., Ma, Z., Kim, S., Hong, J., Park, J., Choi, S., Maeda, M., Shahabuddin, M., Rindfleisch, M., Tomsic, M., Dou, S. Xue. & Kim, J. (2016). Evaluation of persistent-mode operation in a superconducting MgB₂ coil in solid nitrogen. *Superconductor Science and Technology*, 29 1-6.

Authors

Dipakkumar Patel, Md Shahriar Hossain, Khay Wai W. See, Wenbin Qiu, Hiroki Kobayashi, Zongqing Ma, Seong Jun Kim, Jonggi Hong, Jin Yong Park, Seyong Choi, Minoru Maeda, Mohammed Shahabuddin, Matthew A. Rindfleisch, Michael Tomsic, S X. Dou, and Jung Ho Kim

Evaluation of persistent-mode operation in superconducting MgB₂ coil in solid nitrogen

Dipak Patel¹, Md Shahriar Al Hossain¹, Khay Wai See¹, Wenbin Qiu¹, Hiroki Kobayashi¹, Zongqing Ma¹, Seong Jun Kim², Jonggi Hong², Jin Yong Park², Seyong Choi², Minoru Maeda³, Mohammed Shahabuddin⁴, Matt Rindfleisch⁵, Mike Tomsic⁵, Shi Xue Dou¹, and Jung Ho Kim¹

¹ Institute for Superconducting and Electronic Materials, Australian Institute for Innovative Materials, University of Wollongong, Squires Way, Innovation Campus, North Wollongong, New South Wales 2519, Australia

² Busan Center, Korea Basic Science Institute, Busan 609-735, Republic of Korea

³ Department of Physics, College of Science and Technology, Nihon University, Tokyo 101-8308, Japan

⁴ Department of Physics and Astronomy, College of Science, King Saud University, Riyadh - 11451, Saudi Arabia

⁵ Hyper Tech Research, Inc., 539 Industrial Mile Road, Columbus, Oh 43228, USA

E-mail: jhk@uow.edu.au and sychoi07@kbsi.re.kr

Abstract

We report the fabrication of a magnesium diboride (MgB₂) coil and evaluate its persistent-mode operation in a system cooled by a cryocooler with solid nitrogen (SN₂) as a cooling medium. The main purpose of SN₂ was to increase enthalpy of the cold mass. For this work, an *in-situ* processed carbon-doped MgB₂ wire was used. The coil was wound on a stainless steel former in a single layer (22 turns), with an inner diameter of 109 mm and height of 20 mm without any insulation. The two ends of the coil were then joined to make a persistent-current switch to obtain the persistent-current mode. After a heat treatment, the whole coil was installed in the SN₂ chamber. During operation, the resultant total circuit resistance was estimated to be $<7.4 \times 10^{-14} \Omega$ at $19.5 \text{ K} \pm 1.5 \text{ K}$, which meets the technical requirement for magnetic resonance imaging application.

Keywords: Persistent-mode operation, MgB₂, superconducting joint, solid nitrogen, MRI

Introduction

Physicians and surgeons rely critically on magnetic resonance imaging (MRI) scans to diagnose and treat critical injuries and medical conditions. In an MRI system, high, stable ($<0.1 \text{ ppm h}^{-1}$), and uniform ($\leq 10 \text{ ppm}$ in 50 cm diameter of spherical volume (DSV)) magnetic fields are required for obtaining high resolution images of the human body. The unique possibilities for operation of superconducting magnets (i.e., persistent-mode) make them ideal for MRI with a central field strength $>0.35 \text{ T}$ [1]. Thus, in the majority of commercially available MRI systems, superconducting persistent-magnets based on niobium titanium (Nb-Ti) have been used [2]. These magnets, which are cooled in an expensive liquid helium (LHe) bath at 4.2 K, cannot currently be avoided. Thus, the high operation costs of MRI systems obstruct their extensive use in developing and underdeveloped countries [3].

To fulfil the above requirements, the magnesium diboride (MgB_2) magnet, which can be operated at around 20 K in an LHe-free manner, is considered as one of the best potential candidates for next-generation MRI application [4, 5]. It has been reported that the heat capacity of MgB_2 magnets can be significantly enhanced by cooling them using solid nitrogen (SN_2) with a cryocooler [6]. The high heat capacity of SN_2 is well known to enable a magnet to operate for a certain time period in the absence of a cooling source (i.e., cryocooler) [7], which is suitable for areas where power failure is common. Takahashi *et al* reported the first successful persistent-mode coil with joints between MgB_2 and Nb-Ti wires [8]. Jiayin *et al* reported the operating results for MgB_2 persistent-mode coils in a helium environment [9]. Nardelli *et al* also reported on persistent-mode operation with a short MgB_2 tape winding operating with conduction cooling [10]. Until now, however, there have been no reports on persistent-mode operation in an SN_2 cooled system with an MgB_2 coil.

In this paper, the fabrication of an MgB_2 coil and its persistent-current switch (PCS), a newly developed SN_2 cooling system, and the operation of the coil in persistent-mode are presented in detail.

Experimental details

Hyper Tech Research Inc. supplied monofilamentary carbon-doped MgB_2 wire (strand no. 3356) for the coil. The wire was 0.84 mm in diameter, constructed with an MgB_2 filament (diameter – 0.4 mm), a niobium inner barrier (thickness - 0.10 mm) and a Monel outer

sheath (thickness - 0.12 mm). Figure 1(a) presents a digital photograph of the coil, which was fabricated via the wind and react method with a heat treatment at 690 °C for 30 min in argon (Ar) atmosphere. The whole coil was assembled with the main MgB₂ coil at the bottom and the PCS at the top. The PCS was made by extending the two ends of the coil and joining them together. The diameter of the PCS was 113.5 mm with two non-inductively wound turns, and its estimated wire resistance $\sim 7.1 \text{ m}\Omega \text{ m}^{-1}$ at 40 K. The inner diameter and the height of the coil were 109 mm and 20 mm, respectively. The coil was wound in a single layer (22 turns) without any insulation. The calculated inductance of the coil was $86.7 \pm 0.02 \text{ }\mu\text{H}$ [11].

The joining process developed at the University of Wollongong include [12]: (i) etching the Monel from the area of the wires to be joined, (ii) polishing the ends of the two wires until the MgB₂ core was exposed, (iii) aligning the two wires together using glue, (iv) mounting the two wires in a stainless steel (SS) enclosure using a high temperature sealing material, (v) packing the Mg + 2B composite powder in the SS enclosure in Ar atmosphere, (vi) pressing the powder using SS plug, and (vii) sealing the remaining gaps using a high temperature sealing material.

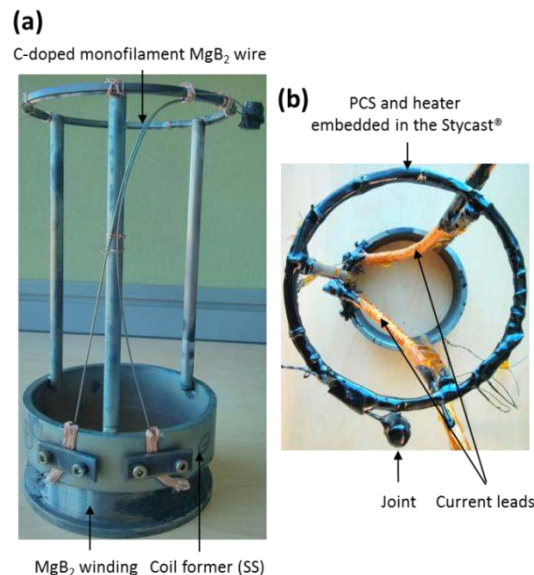


Figure 1. (a) Digital photograph of the fabricated coil after heat treatment, (b) top view of the coil after applying Stycast® 2850 FT (Catalyst 9) epoxy.

To charge the current into the main coil, the PCS was needed to be heated up to resistive state. This was achieved using a 47 Ω Nichrome heater (Lakeshore, 32 AWG) wound on the PCS. Copper (Cu) current leads were installed between the PCS and the coil. Three pairs of

voltage taps were attached, one each from the coil, the PCS, and the joint, to monitor the voltage drops during charging of the coil. A top view of the coil after applying epoxy encapsulant Stycast® is shown in figure 1(b).

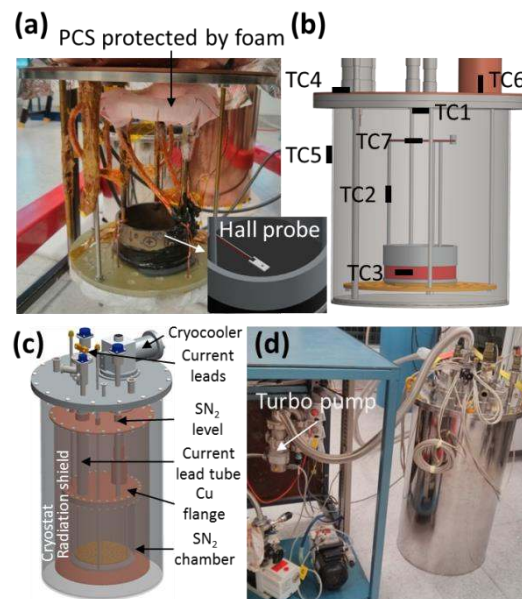


Figure 2. (a) Photograph of the installed coil in the SN₂ chamber, with a 3D model of the Hall probe location (the centre of the coil at $z = 0$) shown in the inset; (b) schematic diagram of the temperature sensor locations (TC1 – at the top of the SN₂ chamber (inside), TC2 – at the centre, between the coil and the PCS, TC3 – at the coil winding, TC4 – on top of the SN₂ chamber near the current lead tube, TC5 –100 mm below the top collar of the SN₂ chamber, TC – 6, at the bottom of the Cu bar below the cryocooler, TC7 – at the PCS); (c) 3D model of the SN₂ cooling system, and (d) photograph of the experimental set-up.

Figure 2(a) shows the coil installed in the SN₂ chamber. Prior to installing the whole coil in the SN₂ chamber, the PCS was covered with expanded polyethylene (EPE) foam to enable easy temperature control under the SN₂ for charging the coil. A Hall probe with 0.1 G sensitivity was installed at the centre of the coil to detect the magnetic field (B) generated by the coil (figure 2(a) inset). Seven cryogenic temperature sensors were also installed to monitor the temperatures of the SN₂ chamber and the coil, as shown in figure 2(b). Figure 2(c) shows a three-dimensional (3D) model of the SN₂ cooling system. The Gifford-McMahon two-stage cryocooler (Sumitomo, RDK-408D2) was used in the cooling system featuring 1st stage cooling capacity of 40 W at 43 K and 2nd stage of 1 W at 4.2 K. Figure 2(d) shows the assembled SN₂ cooling system.

Results and discussion

To cool down the coil in SN₂, the system was first evacuated using a turbo vacuum pump (figure 2(d)). The SN₂ chamber was mechanically sealed using indium wire. A vacuum of $<2 \times 10^{-6}$ torr in the system was achieved, and then liquid nitrogen (LN₂) was introduced into the SN₂ chamber. When the temperature at TC6, as shown in figure 2(b), reached 280 K, the cryocooler was switched on. The purpose of the early switching on of the cryocooler was to avoid the rapid evaporation of LN₂. Once the SN₂ chamber was fully filled with LN₂, both the inlet and the outlet were closed, and a non-return valve was installed. The temperature of the radiation shield remained at 36 K throughout the experiment.

Figure 3 shows the temperature profiles of the SN₂ chamber during the system cool down. The total volume of SN₂ in the chamber was about 16 L. It took about 4.56 days to reach the minimum temperature of 7.2 K in the SN₂ chamber, whereas the temperature on the 2nd stage of the cryocooler reached 4.85 K. Liquid to solid, and solid to solid phase transitions were observed at ~ 63 K, and ~ 35.6 K, respectively. The level of the SN₂ in the chamber reached up to the radiation shield flange (see figure 2(c)). Thus, additional heat conduction was taking place from the SN₂ in the current lead and the SN₂ in the tubes running into and out of the chamber. This might have prevented the SN₂ chamber from cooling down to the cryocooler 2nd stage temperature. The temperature inside the SN₂ chamber remained uniform at around $7.4 \text{ K} \pm 0.2 \text{ K}$. However, the temperatures at the TC4 and TC5 locations were around 11.1 K and 10.2 K, respectively. This clearly indicates the high conductive heat load from the current lead tube (with SN₂) to the SN₂ chamber. In fact, prior to fabricating this system, our finite element method (FEM) simulation predicted similar behaviour even without SN₂ in the current lead tube. The temperature gradient might be due to the lower thermal conductivity of the SS material of the SN₂ chamber. Owing to this, the cryocooler was unable to absorb heat from the far end of the SN₂ chamber. Thus, a 3 mm thick Cu flange was placed on the top of the SN₂ chamber (see figure 2(c)). As a result, the FEM simulation showed a negligible temperature gradient after installing the Cu flange on top of the SN₂ chamber.

However, during actual cool down, due to the high conductive heat load through the SN₂ in the current lead tube, the cryocooler (when at 4.85 K) was unable to absorb heat from the far end of the SN₂ chamber, which left a temperature gradient on top of the SN₂

chamber. On the other hand, when the temperature of the SN_2 chamber was controlled to around 18 K, the temperature gradient in entire SN_2 chamber was reduced to ~ 1.75 K (not shown here), which indicates that the Cu flange facilitated better heat conduction to the cryocooler.

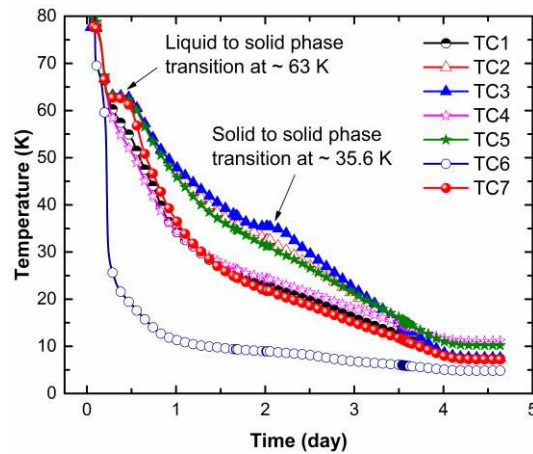


Figure 3. Temperature vs. time profiles during cool down of the SN_2 chamber.

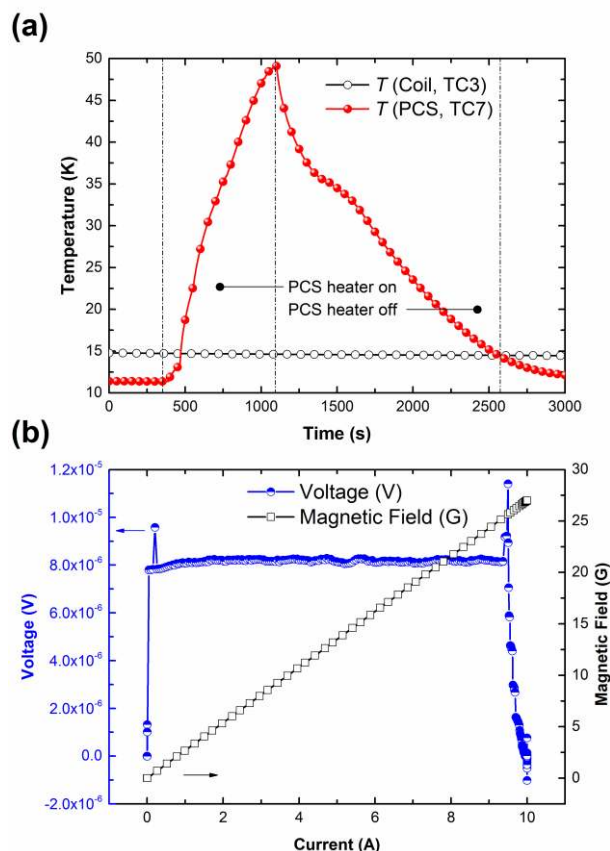


Figure 4. (a) Temperature vs. time profile during open/closed operation of PCS, TC3 – at the coil winding, TC7 – at the PCS, and (b) voltage and magnetic field vs. current profiles while charging the coil when the PCS was open.

PCS testing

The on/off function of the PCS was evaluated at the PCS temperature of 11.3 K. As can be seen in figure 4(a), the PCS reached 45 K in 600 s. The heater power was 3 W. Once the PCS temperature climbed above 45 K, the coil was charged with a ramp rate of 0.1 A s^{-1} up to 10 A. As can be seen in the figure 4(b), B at the centre of the coil was increasing linearly with the current. At 10 A, the B at the centre of the coil was 27 gauss (G), which matched the calculated value of 24.8 G. The variation in B might be due to misalignment of the Hall probe. During current charging, the inductive voltage was about $8.17 \pm 0.12 \text{ } \mu\text{V}$, which is comparable to the $81.7 \pm 1.2 \text{ } \mu\text{H}$ inductance of the coil. This value is well matched with the calculated inductance of $86.7 \pm 0.02 \text{ } \mu\text{H}$. After reaching 10 A, the PCS heater was switched off. It took about 1480 s to cool down the PCS. The reasons for the longer PCS cool down time might be due to over-protection of the PCS, contact between the SN_2 and the PCS (solid phase transition can be seen in figure 4(a)), and lower thermal conduction through the SS bars (see figure 1) from the surroundings to cool the PCS back down to the initial temperature.

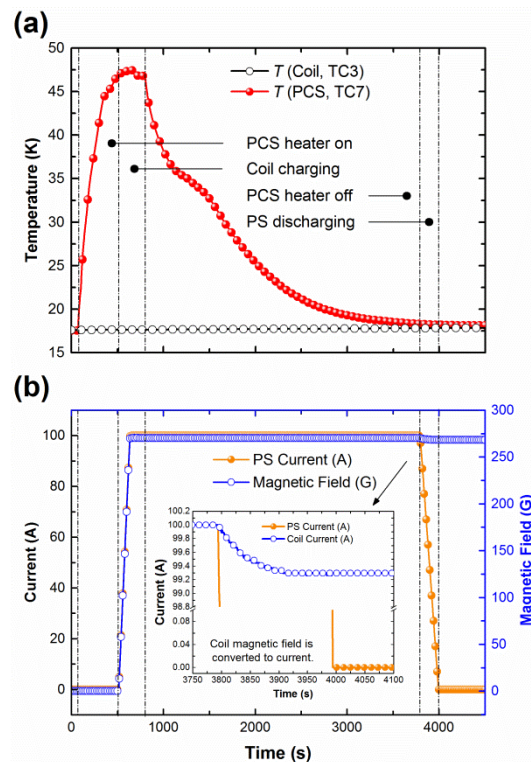


Figure 5. Measurements when the coil was put into persistent-mode at 100 A: (a) temperature vs. time (Coil and PCS) profiles, TC3 – at the coil winding, TC7 – at the PCS, (b)

current and magnetic field vs. time profiles (inset: magnified plot of the current vs. time plot while discharging the PS (coil magnetic field was converted to current)).

Persistent-mode coil testing at 100 A

The temperature of the coil and the PCS was fixed at around 18 K prior to charging the coil. As can be seen in figure 5(a), firstly, the temperature of the PCS was increased above 45 K, and the coil was charged to 100 A with a ramp rate of 0.5 A s^{-1} (figure 5(b)). As can be seen in figure 5(b), we waited for about 140 s and confirmed the coil constant prior to switching off the PCS heater. It took about 3000 s to cool down the PCS. The enthalpy of the material increases at high temperature [11], thus the PCS cooling time was longer at 18 K compare to PCS cooling time at 11.3 K during PCS testing at 10 A. Then, the power supply (PS) was discharged with a ramp-down rate of 0.5 A s^{-1} . To check the initial decay generated by the coil while discharging the PS current, the B in the coil was converted to current using the coil constant. The inset in figure 5(b) shows the magnified profiles of the current vs. time while discharging the PS. Herein, the coil current initially decayed by about 0.7 A, and then remained stable at 99.3 A. Decay in the current showed exponential behaviour. The initial decay might be due to the phenomenon of ‘settling’ of current in closed superconducting circuit [13].

As a result, the coil was kept in the persistent-current mode for about 4.75 days. Figure 6(a) and (b) shows the B and temperature profiles in the coil for the entire persistent-mode duration. In figure 6(a), B was observed to remain around 268.4 G with ± 0.1 G fluctuation, but without any noticeable decay within the resolution limit of a gauss meter. This fluctuation might be due to the data acquisition instrument. During persistent-mode operation, the joint experienced only self-field with very small influence (2.5 G) from the main coil. The temperature of the coil and the PCS was then increased up to 21 K and 20.6 K, respectively (figure 6(b)). If we consider 0.1 G (resolution limit) decay of B in the coil in 4.75 days, the calculated total circuit resistance would be $<7.4 \times 10^{-14} \Omega$ at $19.5 \text{ K} \pm 1.5 \text{ K}$. The B line calculated from the RL circuit time constant corresponding to the minimum measurable resistance of $7.4 \times 10^{-14} \Omega$ over the 4.75 days is also included in figure 6(a). We further need to consider the effect of n -value, indicating a joint quality. It has been reported that the circuit resistance strongly depends on the n -value and joint resistance [11]. Especially, low

n -values make the persistent-mode impossible [14]. Later, the PCS was charged to 200 A without any quench at 20 K. During the attempt to charge the coil to 200 A, a quench occurred when the charging current was 183 A, which damaged the coil. This incident prevented us from carrying out any further experiments. Moreover, in future test, we will implement quench protection system in the experiment to avoid damage to the coil while charging at the higher current.

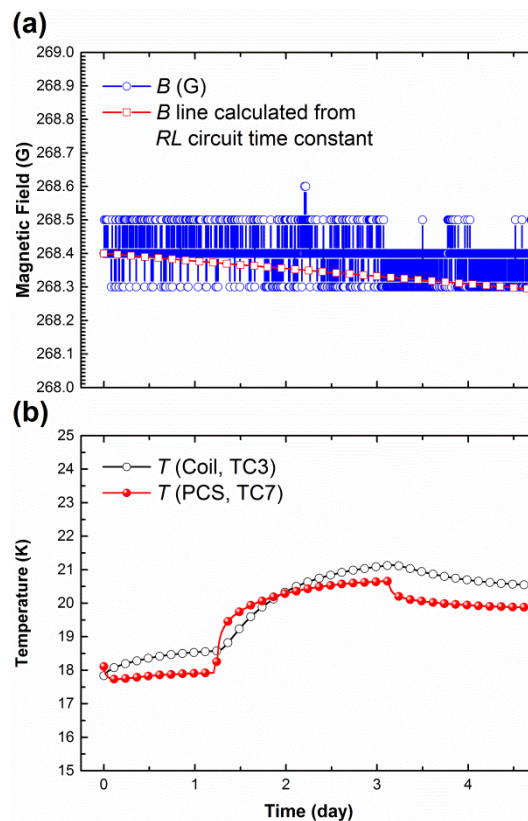


Figure 6. Measurements after putting the coil into persistent-mode: (a) magnetic field vs. time profile of the coil including B line calculated from RL circuit time constant, and (b) temperature vs. time (Coil and PCS, TC3 – at the coil winding, TC7 – at the PCS).

Conclusion

The MgB_2 coil and the PCS were successfully fabricated through a superconducting-joint technique, and the persistent-current mode of the system was evaluated with SN_2 cooling and a 100 A operating current. The total circuit resistance was estimated to be $<7.4 \times 10^{-14} \Omega$ at $19.5 \text{ K} \pm 1.5 \text{ K}$, in the coil during reasonably long-term persistent-mode operation for 4.75 days. This performance is comparable to the technical requirement for practical MRI

application. This joining technique will be further optimized for multifilament MgB₂ conductors in the near future.

Acknowledgments

The authors would like to thank Dr. John Voccio of the Massachusetts Institute of Technology for helpful discussion. This work was supported by the Australian Research Council (FT110100170, DE130101247), University of Wollongong and Australian Institute for Innovative material internal grant, the Korea Basic Science Institute grant number C36222, JSPS KAKENHI grant number 26709021, Deanship of Scientific Research at King Saud University research group project number RGP- VPP-290, and Hyper Tech Research Inc., USA.

References

- [1] Cosmus T C and Parizh M 2011 Advances in whole-body MRI magnets *IEEE Trans. Appl. Supercond.* **21** 2104-9
- [2] Lvovsky Y, Stautner E W and Zhang T 2013 Novel technologies and configurations of superconducting magnets for MRI *Supercond. Sci. Technol.* **26** 093001
- [3] Kara D C 2013 Production of a viable product in magnetic resonance imaging using MgB₂. Master thesis, Case Western Reserve University, 2013
- [4] Modica M, Angius S, Bertora L, Damiani D, Marabotto M, Nardelli D, Perrella M, Razeti M and Tassisto M 2007 Design, construction and tests of MgB₂ coils for the development of a cryogen free magnet *IEEE Trans. Appl. Supercond.* **17** 2196-9
- [5] Mine S, Song H, Xu M, Marte J, Buresh S, Stautner W, Immer C, Laskaris E T and Amm K 2012 Test coil for the development of a compact 3 T MgB₂ magnet *IEEE Trans. Appl. Supercond.* **22** 4
- [6] Bascuñán J, Lee H, Bobrov E S, Hahn S, Iwasa Y, Tomsic M and Rindfleisch M 2006 A 0.6 T/650 mm RT bore solid nitrogen cooled MgB₂ demonstration coil for MRI - A status report *IEEE Trans. Appl. Supercond.* **16** 1427-30
- [7] Yao W, Bascuñán J, Kim W S, Hahn S, Lee H and Iwasa Y 2008 A solid nitrogen cooled MgB₂ "demonstration" coil for MRI applications *IEEE Trans. Appl. Supercond.* **18** 912-5
- [8] Takahashi M, Tanaka K, Okada M, Kitaguchi H and Kumakura H 2005 Relaxation of a trapped magnetic field in a 100 m long class MgB₂ solenoid coil in persistent current mode operation *Supercond. Sci. Technol.* **18** S373-S5
- [9] Jiayin L, Voccio J P, Seungyong H, Youngjae K, Jungbin S, Juan B and Iwasa Y 2015 Construction and persistent-mode operation of MgB₂ coils in the range 10-15 K for a 0.5-T/240-mm cold bore MRI magnet *IEEE Trans. Appl. Supercond.* **25** 1-5
- [10] Nardelli D, Angius S, Capelluto A, Damiani D, Marabotto R, Modica M, Perrella M and Tassisto M 2010 Persistent mode MgB₂ short windings *IEEE Trans. Appl. Supercond.* **20** 1998-2001
- [11] Iwasa Y 2009 *Case studies in superconducting magnets, design and operation issues* (New York: Springer)
- [12] Patel D, Hossain M S A, See K W, Xu X, Barua S, Ma Z, Choi S, Tomsic M and Kim J H 2015 MgB₂ superconducting joints for persistent current operation *Supercond. Sci. Technol.* **28** 065017

- [13] Brittles G D, Mousavi T, Grovenor C R M, Aksoy C and Speller S C 2015 Persistent current joints between technological superconductors *Supercond. Sci. Technol.* **28** 093001
- [14] Patel D, Hossain M S A, Motaman A, Barua S, Shahabuddin M and Kim J H 2014 Rational design of MgB₂ conductors toward practical applications *Cryogenics* **63** 160-5